MOSAIC@ELT: towards final design and AIT development of an athermal camera prototype for the NIR-spectrograph

Tony Pamplona, Zalpha Challita, Johan Floriot, Laurent Martin, Franck Ducret, Kacem El Hadi, Gerardo Veredas, Ana Perez, Marisa L García-Vargas, Éric Prieto, et al.

MOSAIC @ELT: Towards final design and AIT development of an athermal camera prototype for the NIR- spectrograph

Tony Pamplona*[a], Zalpha Challita[a], Johan Floriot[a], Laurent Martin[a], Franck Ducret[a], Kacem El Hadi[a], Gerardo Veredas[b], Ana Perez[b], Marisa L. García-Vargas[b], Eric Prieto[a], Jesús Gallego Maestro[b], Mathieu Puech[c], Roser Pello[a] on behalf of the MOSAIC consortium[⋆]

[a]Aix Marseille Univ, CNRS, CNES, LAM, Marseille, France; [b]Univ. Complutense de Madrid (Spain), FRACTAL S.L.N.E. (Spain); [c]GEPI, Obs. de Paris, PSL Research University, CNRS, Place Jules Janssen, 92195 Meudon, France;

ABSTRACT

MOSAIC is the multi-object spectrograph (MOS) for the ESO 39m European Extremely Large Telescope (ELT) approved to enter phase B beginning 2023. MOSAIC combines visible and near-infrared channels, from resolved stars up to the most distant galaxies, with multi-object and multi-integral field spectroscopy capabilities. The NIR-spectrograph (130K-90K) is one sub-system of the NIR-channel, led by the Universidad Complutense de Madrid (UCM, Spain). It includes four camera modules delivered by the Laboratoire d'Astrophysique de Marseille (LAM, France) and equipped with Teledyne H4RG science detectors (4kx4k, 15 µm pixels). The four modules distribute two identical cryogenic benches ensuring, on each, the spectral coverage of the two observing bands J (0.95 – 1.34 µm) and H (1.43 – 1.80 µm in LR mode and 1.52 – 1.63 µm in HR mode). This paper presents the design of a cryogenic NIR camera prototype based on an athermal concept and details the ongoing AIT development for verification in the 0.95 – 1.34 µm domain in relevant environment (ESO TRL5).

Keywords: Multi-object spectrograph, Extremely Large Telescope, near-infrared cryogenic camera, prototype, athermalization, finite element analyses, assembly-integration-tests (AIT)

1. INTRODUCTION

MOSAIC is the multi-object spectrograph (MOS) for the ESO 39m European Extremely Large Telescope (ELT) approved to enter phase B beginning 2023. The study of the formation and evolution of the galaxies to the most distant ones and of the matter distribution are part of its main objectives ([1] & [2]). Thanks to visible and near-infrared (NIR) channels, MOSAIC will offer multi-object spectroscopy and multi-integral field spectroscopy capabilities. Focusing on the NIR-channel system, its NIR spectrograph sub-system (130K-90K) led by the Universidad Complutense de Madrid (UCM, Spain), includes four camera modules distributed on two similar cryogenic benches and ensuring the spectral coverage of the two following observing bands on each one: J (0.95 – 1.34 µm) and H (1.43 – 1.80 µm in LR mode and 1.52 – 1.63 µm in HR mode). These two cryogenic cameras are parts of the deliveries under the responsibility of the Laboratoire d'Astrophysique de Marseille (LAM, France) and they will be equipped with Teledyne H4RG science detectors (4kx4k, 15 µm pixels). These impressive camera modules have been identified as part of the sensitive modules, like the positioners of the instrument front-end ([3]), that require the development of a prototype. This paper presents the design of a cryogenic NIR camera prototype (scale 1:1 equivalent, diam. ~ ∅400 mm) based on a very compact and innovative athermal concept, able to maintain the focal plane array at the same focus position between integration/tests at ambient and tests/operation at cold (90K) with a precision of few microns. The prototype optical manufacturing is realized in collaboration with Bertin Winlight (Bertin Technologies group, France). It details also the ongoing AIT development for verification in the 0.95 – 1.34 µm domain in relevant environment (ESO TRL5). Firstly, the design of the athermal opto-mechanical assembly and the results in terms of Finite Element Analyses (FEAs) will be detailed; static, modal and thermo-mechanical analyses will be given in terms of first main frequencies, maximum stresses and maximum displacements for the different components. A next part of the paper will focus on the results of a dedicated cryo-mechanical test campaign performed on glued and screwed interfaces identified as critical. Finally, the assembly, integration and verification strategies will be presented.

*Further author information: tony.pamplona@lam.fr; zalpha.challita@lam.fr / http://www.mosaic-elt.eu

*MOSAIC is an international consortium including countries in the core of the project (Partners: France, United Kingdom, The Netherlands, Germany) as well as other participating countries (Associate Partners: Austria, Brazil, Finland, Italy, Portugal, Spain, Sweden, Switzerland, together with University of Michigan and STScI in the USA).

2. CURRENT BASELINE OF THE NIR-SPECTROGRAPHS OF MOSAIC

2.1 Overview of the NIR-Spectrographs

The current NIR spectrograph architecture baseline, driven by the large number of fibers, proposes two separate cryostats installed on the ELT Nasmyth platform, each one enclosing one NIR-Spectrograph. The two spectrographs are twin, working in the same two bands, J and H, and with identical modules. Each one is enclosed in a cryostat, positioned on an aluminum cryogenic bench and oriented so that the two benches and more generally the two cryostats are also twins, as showed in Figure 1. This architecture has evolved since the last year with the evolution of the MOSAIC architecture and volume allocation on the Nasmyth platform and with the finalization of several trade-offs. The Specification and Architecture Review (SAR) is planned between end-2024 and beginning-2025.

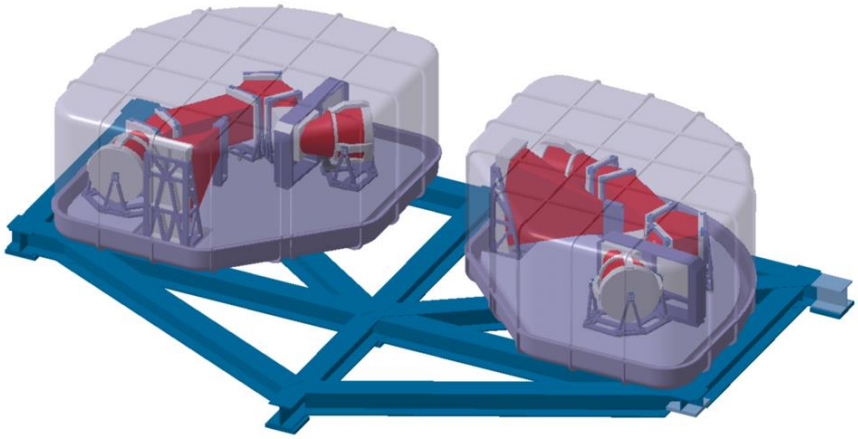

Figure 1. MOSAIC NIR spectrographs on their main platform (current baseline)

The development of the NIR-Spectrographs sub-systems for the MOSAIC instrument NIR-Channel is led by the Universidad Complutense de Madrid (UCM, Spain) and the NIR-Spectrographs optical design is under LAM responsibility ([4]). Figure 2 details the different opto-mechanical modules of the NIR-Spectrographs.

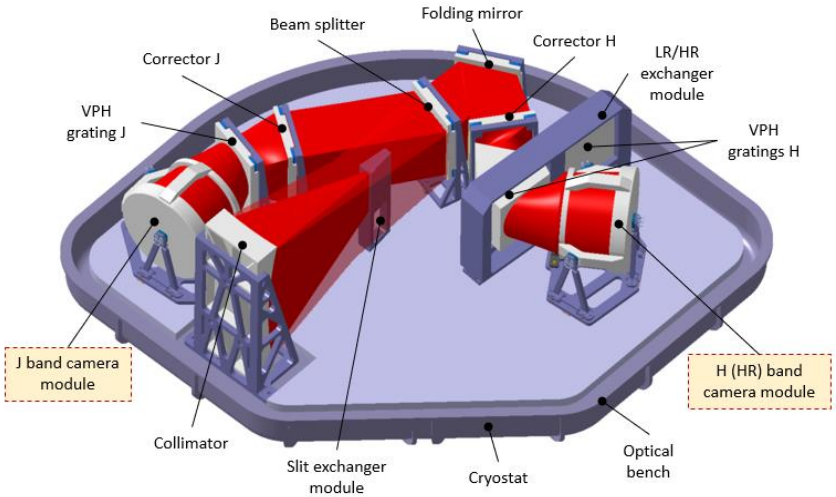

Figure 2. The NIR-Spectrograph layout with its opto-mechanical modules on the cryogenic bench

For each spectrograph, a slit module at the spectrograph entrance delivers the light coming from the fiber bundles inside the spectrograph to the collimator mirror. The slit has a length of 214 mm. The on-axis spherical collimator mirror reflects the collimated beam to a beam splitter separating then the light in two arms, one dedicated to the J-band observations (0.95 – 1.34 µm) and the second one dedicated to the H-band observations (1.43 – 1.80 µm). In each arm, a corrector plate, a VPH module and a camera are present. Each four camera is also equipped with a Teledyne H4RG science detector (4kx4k, 15 µm pixels) to ensure a simultaneous spectral coverage.

2.2 Context and objectives of the prototype development

As described previously, the NIR Channel architecture of the instrument has evolved in order to simplify the design, manufacturing, integration and test phases of the system, and proposes now two sperate cryostats enclosing each one a NIR spectrograph and ensuring a cryogenic environment from 130K to 90K (locally for the detectors). Since the nominal design, observing band I has moved to the Visible channel of the instrument and for the moment two camera modules populates each NIR-spectrograph, one dedicated to J-band and the second one to H-band. In particular, for the H-band, the camera is able to rotate on the cryogenic bench (current baseline) to switch from low resolution LR to high resolution HR mode (1.52 – 1.63 µm), moreover the H-band detector is able to tilt independently (~ 0.14° as current baseline, equivalent to a preliminary estimation of ~ 80 µm of movement), thanks to dedicated cryogenic mechanisms including motors and actuators. On Figure 2, only the camera positioned for the HR mode of H-band is represented.

The design of the camera modules still offers a very compact opto-mechanical assembly based on a Schmidt optical configuration, with a catadioptric system of length ~ 300 mm and diameter ~ 400 mm. This configuration works at ~ f/0.95 and with an expected central obscuration in throughput of less than 20%. Each camera is optimized for its operational observing band. The challenge here is to converge to an innovative athermal and compact opto-mechanical assembly for each camera, able to maintain the focal plane array at the same focus position between integration/tests at ambient and tests/operation at cold (90 K) with a precision of a few microns (objective: ± 10 µm, goal: ± 5 µm). Nevertheless, the focal plane array will be installed on a dedicated assembly offering accessible adjustment ranges for focus and tip-tilt and used during the first steps of alignment, mainly for the compensation of manufacturing and integration residual errors. Once the camera is fully assembled and integrated, the focal plane array is aligned at warm temperature at the required nominal focus position. Before cool down of the NIR-Spectrograph, no manual shimming or motorized readjustment is required thanks to the athermal behavior of the module: the focal plane array focus positioning is maintained until the operational cool temperature. In that way, the differential thermal shrinkage is already calculated and included in the designs, successive thermal cycles to iterate on shims and adjustments are not necessary, motorized adjustments are not necessary and the NIR-Spectrograph final fine tune alignment is not carried by the detector, reducing the duration of the test phase at module level at LAM but also at sub-system and system level at UCM and at instrument AIV level ([7]), the number of manipulations and their inherent risks.

These impressive large cameras have been identified as part of the sensitive modules that require the development of a prototype at an equivalent of scale 1:1 and planned to be in test for the preliminary design review (PDR) and to be delivered at the end of MOSAIC phase B (2026). The main objective of the prototype is the verification of this athermal behavior compliance and its reproducibility in a similar cryogenic environment than the NIR-Spectrograph, allowing to reach the required ESO-TRL5 level. Additionally, the prototype will serve also for verification of the gluing and screwing interface dimensioning, the manufacturability of complex parts, the well functionality of the assembly and integration tools and the associated procedures and the alignment and test strategies with the test benches. The results from this prototype at PDR will also permit the consolidation of the final design review (FDR). As the four cameras are very similar in terms of opto-mechanical concept, the prototype will therefore be representative of all the cameras. Regarding the focal plane array, the option is to use a detector simulator equipped with half spheres and via double-pass optical fibers illumination. The operational temperature profile of the camera is between 130 K and 100 K for the optical block and 90 K at the focal plane array. The thermal stability of the camera is ensured by the selection of very similar optical and mechanical materials in terms of coefficients of thermal expansion to obtain a full assembly as homogeneous as possible. An additional non-negligeable aspect is that the development of the prototype AIT tools is realized trying to reduce as much as possible the number of components and their complexity and also trying to anticipate and to recycle as much as possible the tools and procedures, in the perspective of the science cameras.

3. PROTOTYPE OPTICAL DESIGN

3.1 Prototype optical layout description

Like the science camera modules, the camera prototype is a ~ f/0.95 Schmidt system with a catadioptric architecture inherited from the one of MOONS ([6]). The optical layout is detailed on Figure 3 and includes the object plan (equivalent to the slit in the NIR-Spectrograph with length of 214 mm) and an on-axis spherical collimator mirror working at f/3.47. The prototype is optimized in the J spectral band (0.95 – 1.34 µm) and more precisely between 1.0 – 1.37 µm. The focal plane simulates the science one with 60.1 x 60.1 mm² of dimension, equivalent to a 4kx4k H4GR detector with pixels of 15 µm. The pupil here is located at 1500 mm in front of the first surface of the camera prototype (150 mm for the science camera) and presents a diameter of 260 mm, according to the clear aperture of the optical window of the cryostat used for the tests and verification. The full length of this compact optical system is ~ 300 mm. As shown on Figure 3, the slit and the spherical collimator used during the prototype assembly-integration-tests phase (AIT phase) are placed outside the cryostat, at warm temperature.

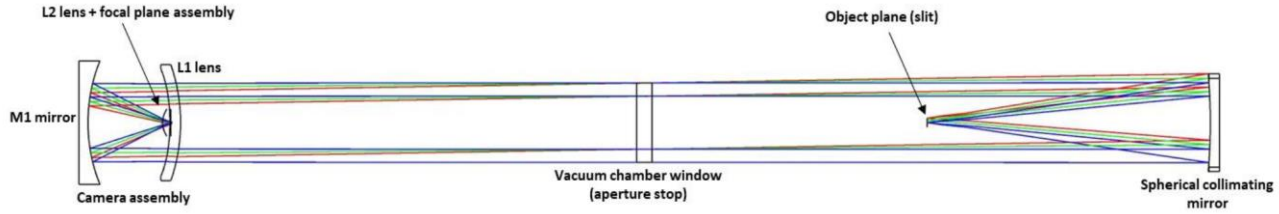

Figure 3. Optical layout of the camera including the slit and the spherical collimator

The lens L1 is a meniscus lens with a concave aspherical surface with a clear aperture of 300 mm of diameter. At its center, a rectangular hole of 90 x 90 mm² allows the integration of the lens L2. It generates a central obscuration of ~ 11 % on the throughput for this prototype. The mirror M1 is an aspherical concave collimator with a circular clear aperture of 315 mm of diameter. The field lens L2 is a plano-convex lens with an aspherical surface. L2 is embedded in L1 with bonding interface. The beam coming from the slit and the collimator crosses the cryostat window and the prototype lens L1; L1 then transmits the beam to the prototype mirror M1 and M1 reflects the beam to L2. The beam is finally focalized on the focal plane array, at 3 mm after L2 exit surface. Due to the compactness of the opto-mechanical assembly, the distance between L2 and the focal plane is very short and the remaining space for integration and stray light control and optimization is very small. M1 mirror is in Quartz with protected silver coating; L1 and L2 are in Fused Silica with an anti-reflection coating able to transmit in J-band and in the Visible for alignment steps at warm. The distance between L1 and M1 is ensured by struts in Quarts. For the science cameras, Quartz material will be replaced by Zerodur.

Optical manufacturing and L2/L1 bonding will be performed is collaboration with Bertin Winlight (Bertin Technologies group, France) and will be defined in a way to ensure a perfect assembling and alignment of the components.

3.2 Prototype optical quality

Even if the most of the optical surfaces of the camera prototype are aspherical, their sags and slopes remain standard aspherical components avoiding more complexity in terms of manufacturing and tests.

Figure 4 represents the spot diagrams obtained in the J-band and for different wavelengths and Field of View (FoV) positions; spot diagrams at 633 nm are also presented showing that measurement in Visible during the test phase is possible, if necessary and additionally to visual alignment with Visible light; a comparison between prototype at warm and prototype at cold (90K at the FPA) is given. Here the prototype is optimized taking into account AIT equipment functional wavelengths (for NIR and VIS), so the spot diagrams obtained are different than the ones of the final J-Band science camera of the instrument. The image quality is not perfect but sufficient for measurement and verification of the athermal behavior of the prototype between warm and cold environment which is the main objective of this prototyping phase. Another aspect is that the optical architecture of the camera is not very sensitive to misalignments as described in Table 2 showing the alignment sensitivities of the different optical components leading to acceptable degradations of EED-80.

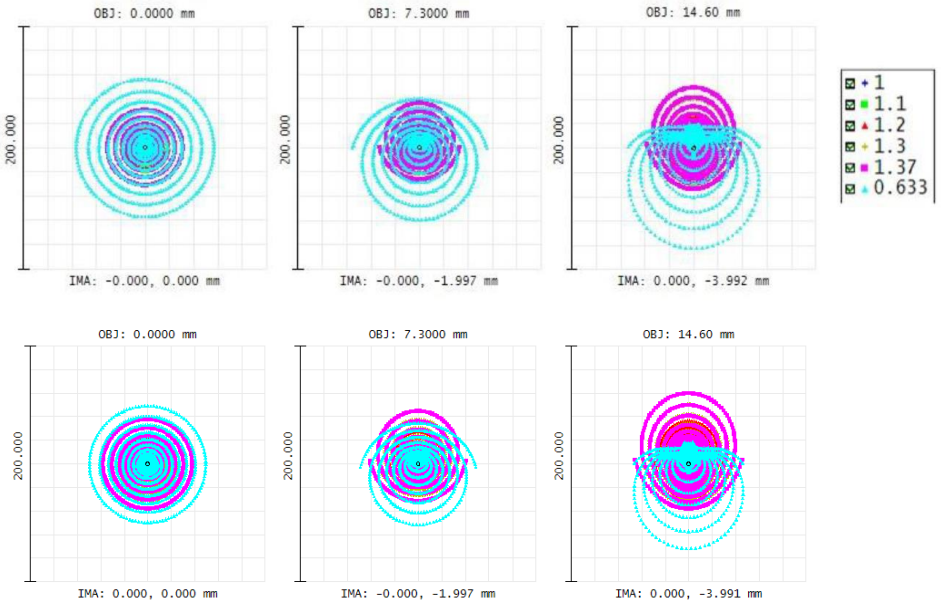

Figure 4. Spot diagrams obtained at the system focal plane, in Visible and J-band wavelengths. Top: at warm. Bottom: at cold.

Table 1 gives the values of the 80% encircled energy diameters (EED-80) at 1.2 µm and at 633 nm wavelengths and for several positions in the field. Values at ambient and cold temperatures are considered.

Table 1. Table 1. EED-80 values for several positions in the field, at image plane and for 1200 nm and 633 nm (1 px ≡ 15 µm)

Field position (mm)	**EED - 80% at 1.2 µm @$T_{amb.}$ [T_{cold}]**	**EED - 80% at 633 nm @$T_{amb.}$ [T_{cold}]**
0.0, 0.0	1.1 px [0.98 px]	2.4 px [2.3 px]
0.0, 7.3	1.6 px [1.2 px]	2.6 px [2.2 px]
0.0, 14.6	2.4 px [1.6 px]	3.1 px [2.2 px]

Table 2. Sensitivity to alignment errors. The values in parentheses give the degradation of the 80% encircled energy diameter.
*De-space error could be compensated by a refocusing adjustment of the focal plane.

	Lateral decentering	**Tip-tilt**	**De-space***
Between L1/L2 assembly and M1	200 µm (6 %)	2.4’ (8 %)	10 µm (6 %)
Between L2 and L1	500 µm (6 %)	30’ (6 %)	10 µm (8 %)
Of the focal plane	-	7’ at edge (10 %)	10 µm (8 %)
Between the whole camera and the incident beam	3 mm (2 %)	18’ (2 %)	50 mm (< 0.1 %)

This table confirms that the alignment tolerances of the camera are quite loose. This is a very strong advantage of this Schmidt catadioptric design. De-space movement is the most critical degree of freedom but it will be compensated by the athermal nature of the design (monolithic structure and athermal design of the focal plane assembly); if necessary, an additional (expected to be smaller) could be made thanks to the adjustment of the focal plane position along the optical axis (refocusing by shimming for example). The whole camera positioning with respect to the incident beam is loose due to the fact that the incident beam is collimated.

Table 3 gives the manufacturing sensitivities of the different optical components leading to acceptable degradations of EED-80: the thickness sensitivity of L2 lens is critical but it can be compensated by the refocusing of the focal plane; radius of curvature (RoC) sensitivities are quite tight, particularly for M1, but are expected to be achieved by manufacturers; it mainly introduces defocusing of the camera and it can be compensated by refocusing if necessary; centering, wedge and surface irregularities sensitivities are relatively loose and easily achieved by standard polishing.

Table 2. Sensitivity to manufacturing errors. The values in parentheses give the degradation of the 80% encircled energy diameter.
*Thickness errors could be compensated by a refocusing adjustment of the focal plane.
**Surface irregularities should be understood has low-frequency pattern surface form errors (astigmatism, coma, trefoil and spherical aberration contributors)

Optical components	**Sensitivities on**				
	Thickness*	**RoC**	**Centering**	**Wedge**	**Irregularities****
L1	250 µm (8%)	0.1% (23%)	200µm (9%)	3’ (9%)	λ/3 RMS at 633nm
L2	10 µm (9.5%)	0.2% (5%) for curved surface < 15µm residual sag for flat surface	500µm (6.5%)	30’ (9%)	λ/2 RMS at 633nm
M1	-	0.05% (7%)	-	-	λ/5 RMS at 633nm

4. PROTOTYPE OPTO-MECHANICAL INTERFACES AND THERMAL CONSIDERATIONS

4.1 Overview of the current opto-mechanical architecture and interfaces

The science cameras of the NIR-Spectrographs present three main assemblies: i) the optical assembly including the mirror M, the two lenses L1 and L2 and the four structural struts (manufactured in a similar material than the mirror) ensuring the optical maintaining and the rigidity of the assembly during handling and shipping; ii) the mechanical assembly including the bipods, the base-plate, the thermal interface (cold arm ensuring the cooling of the electronics and detector) and all their interface mechanical parts; iii) the detector assembly including baffle, cold plate, electronic box, focus and tip-tilt adjustments and the focal plane array (FPA) itself with its own parts.
As shown on Figure 5, the camera prototype is designed with the same architecture.

The optical assembly is glued and screwed on three bipods ensuring a thermomechanical decoupling between the optical components and their environment. Lens L2 is embedded inside lens L1 and glued at its centre. The four struts are also glued on mirror M1 and lens L1 edges. The focal plane array of the detector is installed on its cold plate at the rear of the lens L1 and the local assembly includes a mechanical chain specially calculated to ensure the camera module athermalization and so the maintaining of the focal plane array at the same required position at warm and during/after the cooling down. The FPA is cooled down to 90K thanks to a thermal interface, as a cold strap, designed and optimized to minimize its contribution to the central obscuration. The whole assembly is screwed on a base-plate in Aluminium allowing the module positioning on the NIR-Spectrograph cryogenic bench.

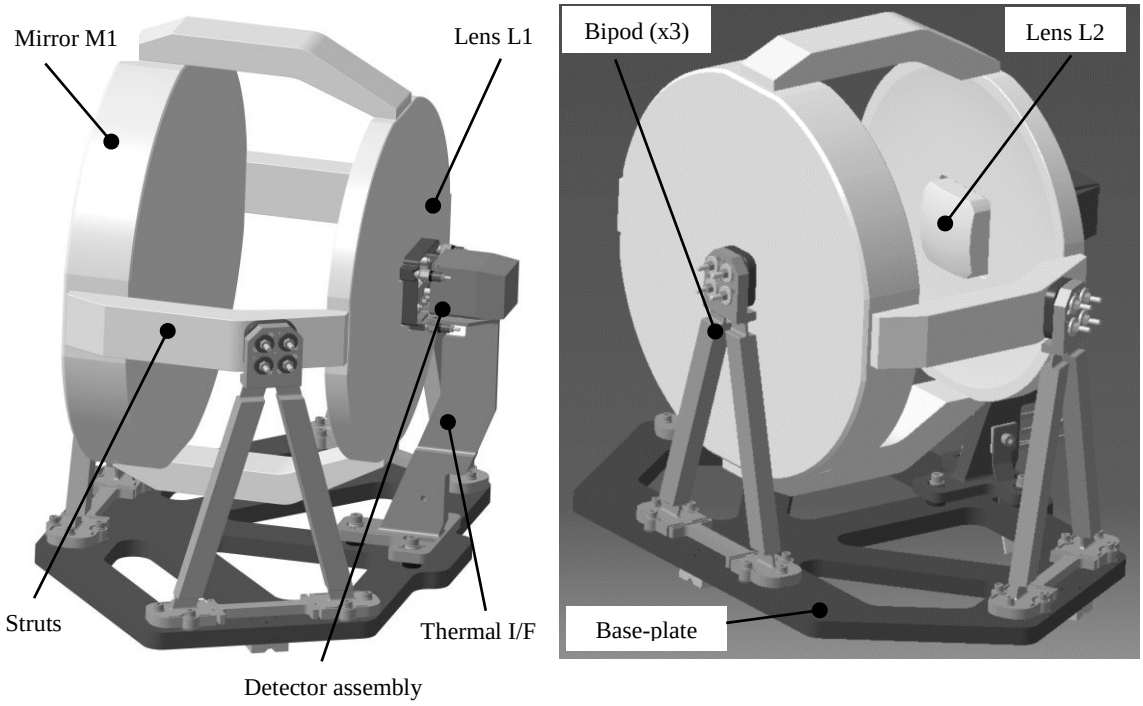

Figure 5. CAD views of the athermal camera prototype

The opto-mechanical design of the NIR-Spectrographs including the science cameras must be compliant with earthquake consideration equivalent to 3g in all directions during operation in cryogenic environment between 90K and 130K, which is a major technical challenge. The camera prototype is also developed according to this specification. The mechanical design is original in that it minimizes the number of mechanical parts required to hold the optical assembly. The ratio of support mass to supported mass is ~ 1:15 without the base-plate.

4.2 Thermal considerations on the mechanical assembly

This section describes the detailed design of main opto-mechanical parts and connections of the camera prototype. The classical technical challenge for an optomechanical assembly operating at cryogenic temperatures is to manage the thermal expansion coefficient differences leading to differential shrinkage of materials constituting the assembly, as explained in the previous section. To manage this phenomenon, main mechanical parts are equipped with flexures systems ensuring thermo-mechanical discoupling between materials used.

Design of the bipod bodies and of detector assembly parts

To manage the phenomenon of differential thermal expansion, the bipods are also designed including thermal blades to ensure thermo-mechanical decoupling between the optical assembly and the cryogenic bench in Aluminium where the prototype (or the science camera) will be set during operation. A set of thin blades is used to manage the radial thermal shrinkage between the optical assembly in Silica or equivalent and the cryogenic bench in Aluminium. Another set of thin blades is used to manage the thermal shrinkage between the Titanium bipod base and the Aluminium base-plate. Each bipod is manufactured in a monolithic Titanium blank. The base of the bipod ensures the required stiffness to achieve the required manufacturing tolerances and to facilitate bipod assembly and integration on the optical assembly and on the base-plate. Several parts of the detector assembly are also designed with the same thermal blade concept. Indeed, this assembly is mounted on an Invar baffle directly glued at the centre of lens L1. Thus, the Invar baffle is equipped with thin blades ensuring the thermal shrinkage of the baffle while minimizing stresses induced on silica lens L1. In the same way, the detector FPA is mounted on an Invar cold plate bolted on the baffle and also equipped with three thin blades at 180° from each others, ensuring a maximal rigidity of the system.

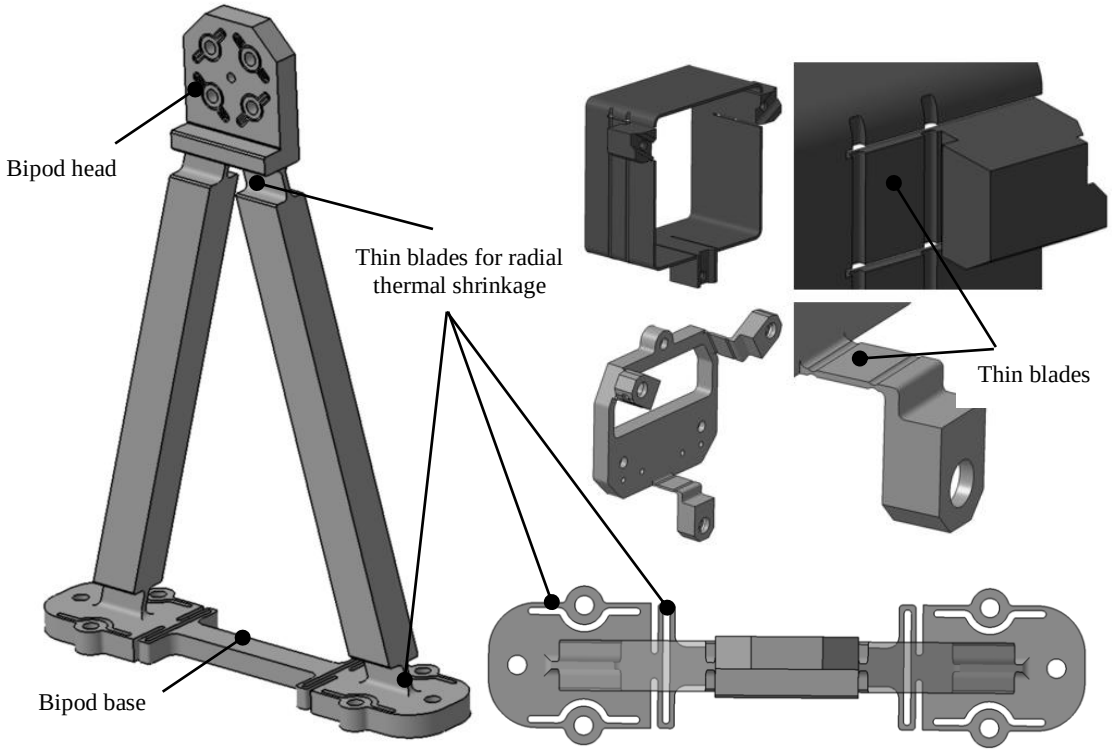

Figure 6. Detailed design of the camera prototype bipods and of several detector assembly parts

Design of the bipod heads and struts

The 35 kg Fused Silica and Quartz (Zerodur for the final science cameras) optical assembly is carried by 3 bipods in Titanium. These bipods support the optical assembly weight in operation and during potential earthquakes, also ensuring that it remains in a stable position during operation. The top of the bipod is called bipod head. One of the main technical challenges is the complexity of attaching this quasi-isostatic system to the optical components. The design of the 3 main attachments is based on the introduction of 3 Invar heads bonded at specific locations on the optical assembly. The bipod heads are then pinned and screwed onto these interfaces. The Invar interfaces and the bipod heads are represented on Figure 6.

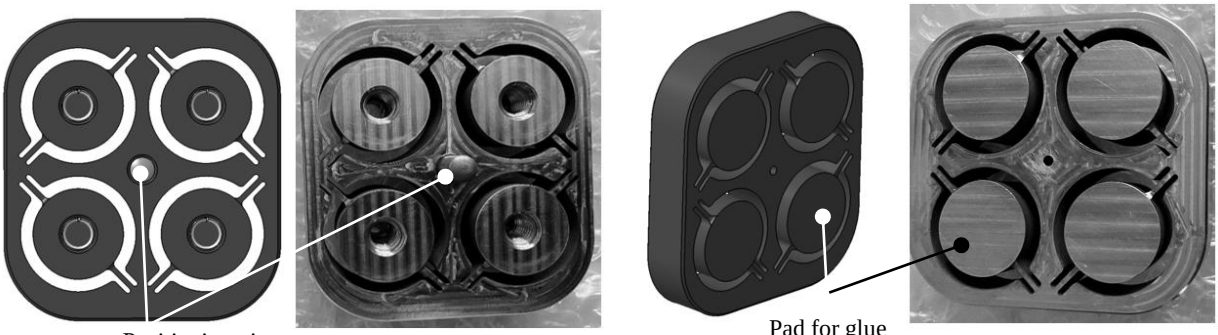

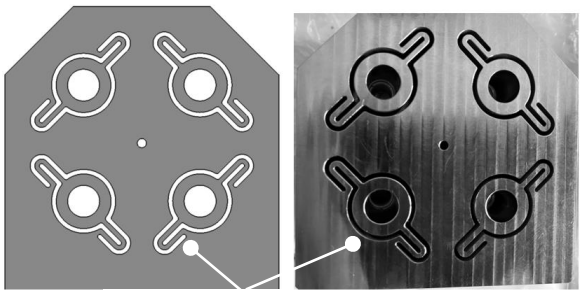

Figure 7. CAD views versus the manufactured Invar interfaces screwed at the top part of the bipods, also called bipod head, (top figures) and CAD views versus the bipod heads in Titanium (bottom figures).

To manage the effects of differential expansion between the different materials involved, flexible flexures are designed on all the interface parts in Invar. The first stage of each link is a bonded connection between the Invar interface and the optical assembly. Invar was chosen because its coefficient of thermal expansion is relatively close to the one of the Fused Silica and of the Quartz (or Zerodur). Despite this compatibility, on the one hand, the diameter of the zones in contact remains limited due to these differential expansion effects; on the other hand, the mass of the optical block is relatively high. As a result, several bonding zones were chosen for the design. Flexible blades manufactured by EDM machining on the Invar interfaces enable the differential thermal expansion between Fused Silica and Invar or between Quartz and Invar, at two bonding zones of the optical assembly. The number of bonded zones is determined by the inertia required to support the weight of the optical block under potential earthquakes. These three Invar interfaces have already been manufactured with success according to CAD design and required manufacturing accuracy as showed on pictures opposite.
The second stage of each connection is the screwing of the bipod head on the Invar interface. Flexible blades machined by electro discharge machining into the Titanium bipod heads manage the differential expansion between Fused Silica and Invar or Quartz and Invar. Pin allows a thermal expansion of the bipod head around it to be controlled. Representative samples of bipod heads have already been manufactured with success according to CAD design and required manufacturing accuracy as showed on pictures opposite.

Other bonded interfaces are used to maintain the mirror and the lens on the horizontal struts in Quartz (or in Zerodur for the NIR-Spectrograph science cameras). These bonded joints are composed of four pads of glue on the mirror M1 side and two pads of glue on the lens L1 side. The differential shrinkage effect can be easier managed because the materials involved in these connections are Fused Silica (L1) and Quartz (struts) or Quartz (M1) and Quartz (struts), so with coefficients of thermal expansion very close to each other.

4.3 Finite Element Analysis

The design of each metallic part of the prototype has been validated with a complete Finite Element Model built with PATRAN/NASTRAN software. Regarding the deformation of the optical surfaces and the thermal calculations of the whole module, preliminary results are described in [] and no major evolution is highlighted with the design evolution. The most stressed parts as flexures have been rigorously analysed. Stresses in glass components have been also evaluated. Maximum stresses in these components appear at bonded locations. Despite of detailed Finite Element Model, a tests campaign is needed to validate the desgin of these connections (see section 4.4). At this stage, the results show that the prototype can achieve basic classical requirements for this kind of cryogenic application as stiffness and strength.

Figure 8 show the Von Mises stresses repartition in the bipods and the baffle of the detector assembly. Maximum stress occurs at the thermal flexure and blade locations. The associated table shows the maximum stress reaches 214 MPa for the bipods and 46 MPa for the baffle; taken into account the required factors of safety for metallic parts, margins can be highlighted. It has to be noted that some of the designed flexures and blades can be very thin (0.4 mm) and their manufacturability has been checked with manufacturers.

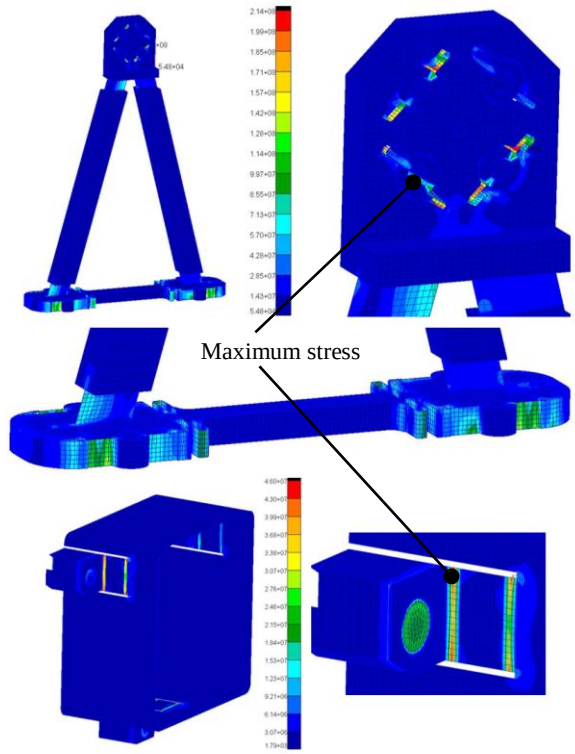

Figure 8. Von Mises stresses repartition on main bipods and baffle

Table 3. Maximum stress and margins obtained on the baffle and bipods

Parts	Stress (MPa)		MOSY (*)	MOSU (*)
	Seism case	Op. case		
Baffle	46	27	3.5	6.2
Bipods	214	130	2.4	2.3

(*) MOSY/U: Margin of safety on yield/ultimate strength

Figure 9 shows the maximum stress repartition in the different glass parts constituing the optical assembly. The maximum stress occurs at bonded joints location and is very local. The associated table shows Maximum local stress is in the order of magnitude equivalent to 20 MPa; taken into account required factors of safety for glass parts, margins can also be highlighted here.

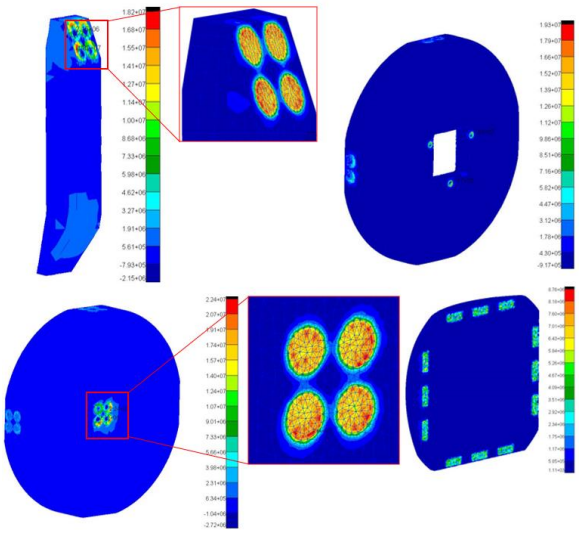

Figure 9. Stresses repartition on glass parts

Table 4. Maximum stress and margins obtained on the baffle and bipods

Parts	Stress (MPa)		MOSU (*)
	Seism case	Op. case	
Mirror M1	22.4	15	0.4
Lens L1	19.3	16.8	0.7
Lens L2	8.8	7.7	2,7
Struts	18.2	15.1	0,8

(*) MOSU :Margin of safety on ultimate stregnth

4.4 Dedicated test campaign on thermomechanical verifications

Test samples representing the bipod heads, Invar interfaces and Silica parts, glued or screwed

In addition to Finite Element Analysis, the complexity of such bonded and bolted interfaces requires a dedicated test campaign to validate their resistance to cryogenic temperatures, as well as their resistance to mechanical stress. This test campaign involves the manufacturing of test samples representative of these interfaces, allowing also the validation of the manufacturability of the thermal flexures. Figure 10 gives examples of the samples used during the test campaign.

The manufactured samples for the test campaign are representative of the glued interfaces of the prototype and of the NIR-Spectrograph science cameras. A first set of samples represents the glued and bolted interfaces between the bipod heads and the optical assembly, including the silica-Invar gluing and the Titanium-Invar bolting. The second set of samples represents the gluing at the ends of main silica struts. The used glue is the structural epoxy bi-component EA9323-2. Six silica-silica samples and three titanium-Invar-silica samples have been manufactured. The first main step of the test campaign was dedicated to prepare a gluing procedure in order to master the gluing of samples. Tests were carried out on Plexiglass samples to estimate the duration of such operation and be in line with recommendations for using adhesive, define the required glue volume to obtain the target diameter of each pad. Then, the procedure was applied on the representative samples (Silica and Invar parts).

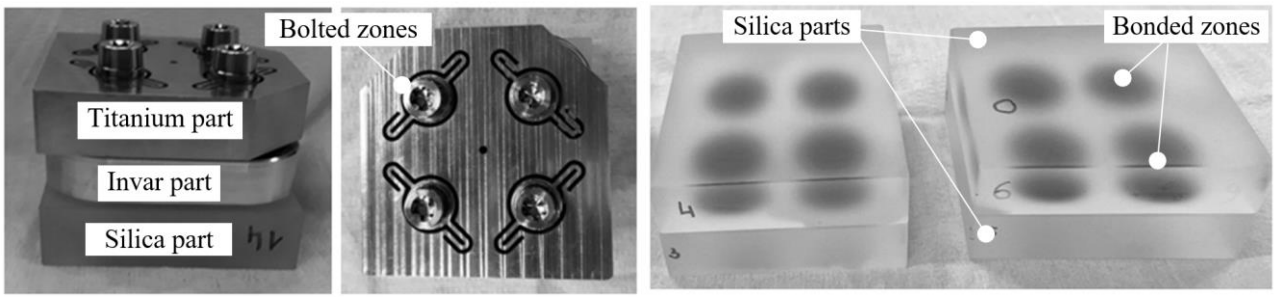

Figure 10. CAD views of representative samples used for thermomechanical validation campaign

Thermal cycling of the test samples

Three of the six bonded Silica-Silica samples and one Titanium-Invar-Silica sample have experienced three thermal cycles in liquid nitrogen, from ambient temperature to 77K (equivalent to -200°C). Figure 11 shows the simplified setup and the measured temperatures with PT100 and thermocouple probes used during the tests. After visual inspection, all the tested samples have conserved their full mechanical integrity with no ungluing or breakage.

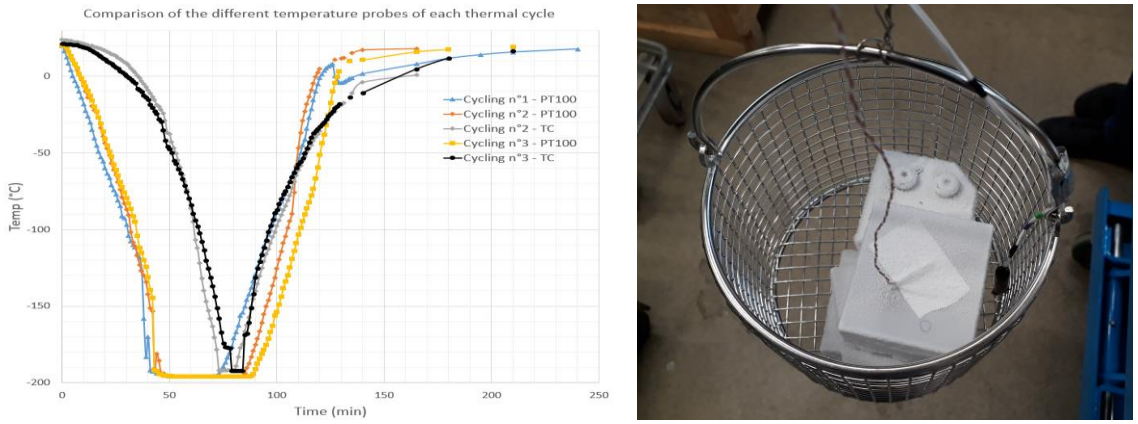

Figure 11. Left: Thermal cycling profiles applied to the samples. Right: simplified setup using liquid Nitrogen

Mechanical resistance of the test samples

After the thermal cycling step, six Silica-Silica samples (3 cycled and 3 non-cycled) and three Titanium-Invar-Silica samples (1 cycled and 2 non-cycled) have experienced mechanical resistance tests on a tensile testing machine. Tests are based on compression load that implies shearing but also tensile effects due to cantilever between applied load and bonding pads. Specific mechanical interfaces have been developed to test the samples.

Each sample underwent three loading cycles up to 5,000 N. After visual inspections, the main result was the mechanical integrity of all samples. One sample even withstood a load of 10,000 N without any damage in the bonded zones, without sliding and without deformation of the thermal flexures. By comparing the results between samples that have undergone thermal cycles and those that have not, the thermal cycles appear to have no impact the behavior of the samples and of all the bonded interfaces.

Fig. 12. Representative samples mechanical tests

By performing Finite Element Analysis on the whole prototype, estimated loads through the mechanical links reach 969 N with a cantilever of 12.1 mm for Silica/Silica interface and 421 N with a cantilever of 26.7 mm for Silica/Invar/TA6V interfaces. Each Silica/Silica sample withstood the 5,000 N load cycle (x3) with a cantilever of 15.15 mm and each Silica/Invar/TA6V sample withstood the 5,000N load cycle (x3) with a cantilever of 27. 4 mm. Thus, mechanical tests highlight high margins in terms of strength for these glued and screwed interfaces. Modified using the same cantilever, loads can highlight margins of 5.5 and 11.2 respectively. The following graphs show the behavior of the samples with the evolution of the applied load. The profiles of the curves are very linear without accident meaning that the glued and screwed interfaces have remained intact throughout the compression cycles, without any start of failure or breakage.

These mechanical resistance tests were performed with the French Laboratoire de Mécanique et d'Acoustique (LMA, Marseille, France).

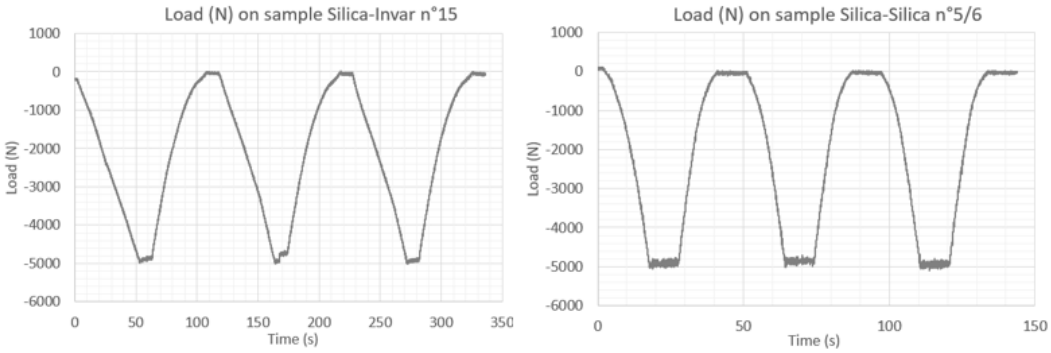

Fig. 13. Load evolution with cycles on representative samples mechanical tests

5. CAMERA PROTOTYPE ASSEMBLY AND INTEGRATION TOOLS

5.1 Assembly and integration tools development

Given their weight and dimensions, assemble the optics to form the optical block, and then assemble this block to its mechanical mount, is a very complex operation. These assemblies have to be performed with a positioning accuracy of the order of magnitude of ± 50 µm with the M1 mirror as reference. The detector assembly is excluded from this study. Dedicated mechanical tools have been designed for these alignment operations. This section describes the strategy of the camera prototype assembly and integration steps. Even with a final adjustment capacity, each alignment step needs an accurate positioning to obtain a final prototype assembly that is as close as possible to the theoretical one and so that its thermomechanical behavior can be controlled as effectively as possible. The design of the dedicated mechanical assembly and integration tools (A&I tools) has been done, based on safe and stress-free holding and manipulations for the optical components.

Several phases of the assembly consist in several gluing illustrated on Figure 14: the mechanical interfaces in Invar on mirror M1, lens L2 inside lens L1, Invar baffle on lens L1 and the four struts on M1 and L1 sides. All these gluing will be performed at LAM except the gluing of L2 in L1 which will be realized at Bertin Winlight (Bertin Technologies group, France) thanks to their expertise with this kind of gluing already developed for the MOONS/VLT instrument ([6]).

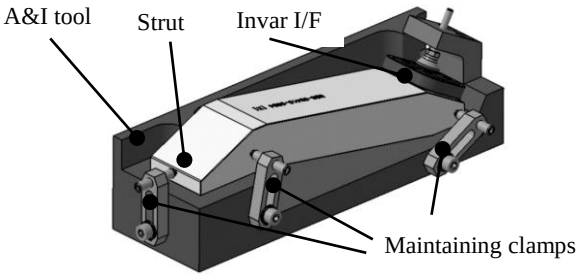

An Invar interface (Invar I/F) is aligned and glued on each Quartz strut via an isostatic mounting ensuring an interface positioning accuracy of ± 20 µm thanks to the manufacturing accuracy of the dedicated assembly tool. The exact location of the Invar interface on the strut is not yet confirmed and the tool is able to adapt the required location.

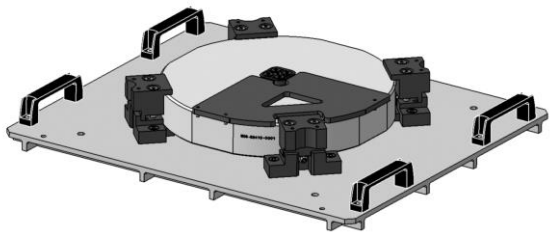

An Invar interface is aligned and glued on mirror M1 back via an isostatic mounting ensuring also an interface positioning accuracy of ± 20 µm thanks to the manufacturing accuracy of the dedicated assembly tool.

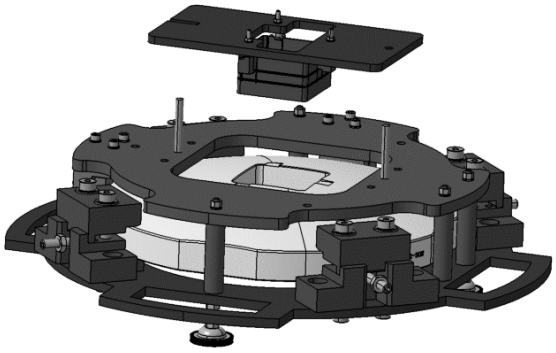

After gluing of L2 inside L1, the Invar baffle is then positioned and glued on lens L1, ensuring a correct relative positioning of the baffle versus lens L2 with lens L1 as reference.

Figure 14. Invar interfaces, lens L2 and baffle gluing with their dedicates A&I tools

Another main phase is the assembly of the optical components and their positioning thanks to dedicated alignment tools. The first step of this phase consists in mounting the upper part of the alignment tool around lens L1 (already equipped with lens L2 and the Invar baffle). In a second step, a specific tool is used to align L1-L2 with the mirror M1. When the alignment is realized, four main struts are glued on M1 and L1 to ensure the required distance between the two components and the structural maintain of the assembly. The mechanical assembly and integration tools shown on Figure 15 is a vertical alignment support ensuring an optimal accessibility for the gluing of the four struts, according to the gluing procedure defined with the test campaign described previously (see section 4.4).

Figure 15. Assembly, alignment and integration of the optical components and the struts.

Then, in a third assembly phase, the alignment tool is dismounted and the optical block is positioned horizontally to allow integration and positioning of the different mechanical interfaces of the system: mount baseplate, bipods and thermal interface.

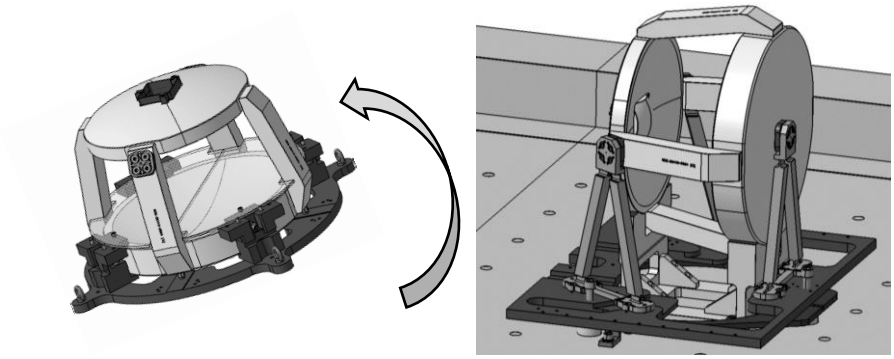

Figure 16. Assembly, alignment and integration of the bipods, the base-plate and thermal interfaces

The last operation concerns the alignment of the detector assembly. In this step, the cold plate equipped with the science focal plane array, or with an equivalent dummy equipment, is positioned and bolted on the baffle. This operation is highlighted as a critical operation due to the required positioning accuracy of the detector relative to the optical assembly better than ± 5 µm from the nominal best focus. The development of a dedicated alignment tool is ongoing.

6. CAMERA PROTOTYPE TEST BENCHES DEVELOPMENT

The main objective of the camera prototype is to demonstrate its athermal behavior in relevant environment, according to ESO TRL5. This relevant environment significates a similar environment than the ones of the MOSAIC science cameras inside the NIR-Spectrograph cryostat, with a temperature reaching 130-100 K for the opto-mechanical assembly and 90 K for the detector FPA. The athermal behavior reproducibility over several thermal cycles needs also to be included in the demonstration for a complete verification of the associated concept, designs and calculations. After the full assembly, integration and alignment of the prototype, a test phase will be performed using two dedicated test benches, one optical test bench and one thermal test bench. Their developments are in progress and their procurements is planned to start beginning 2025.

6.1 Thermal test bench preliminary concept

To test the camera prototype in relevant cryogenic environment, the team will benefit from the ERIOS cryostat facility of the Laboratoire d'Astrophysique de Marseille (LAM, France). This cryostat of 45 m^3 of internal volume has a diameter of 4 meters per length of 6 meters ([8]).
To reproduce the identical thermal environment of the cameras in the MOSAIC NIR-Spectrographs, in particular the temperature gradient from 130K on M1 mirror, 110K on L1-L2 lenses and 90K on the focal plane array, the development of a dedicated thermal test bench is necessary and is in a preliminary design phase. Figure 17 shows a view of ERIOS in the ISO8 integration hall of LAM and a very preliminary concept of the thermal test bench inside the cryostat. The camera prototype will be supported by the ERIOS bench with the same interfaces than in the NIR-Spectrograph cryostat in terms of material and fixation supports. Shields are not yet represented but they will be present and they will allow the required temperature gradient on the module. The optical beam for the tests will cross the cryostat by one of its tapping where a custom optical window will be installed and selected according to the needs for the optical alignment and test, at warm and cold and also in Visible and NIR (J-band) wavelengths. The optical test bench itself will be fully installed outside the cryostat and will have in particular an AIT slit module and an AIT collimator module (see section 6.2) not identical but adapted from the ones of the MOSAIC NIR-Spectrographs.

Another aspect concerns the thermal stability of the whole science camera modules during operation. The current baseline is to not use thermal regulation loops and so the camera prototype will not be thermally stabilized during the test phase inside ERIOS. For this reason, the camera prototype will be also tested in "long duration" cryogenic to verify and quantify the focus and the Point Spread Function (PSF) form stability and their eventual evolutions. Preliminary optical calculations with Zemax, taking into account the materials and CTEs, show that local temperature variations of less than 10 K induce drifts of the focal plane array position of less than 1 µm rms. This result remains largely acceptable since the EED-80 degradation stays also quite negligible. Nevertheless, the tests in ERIOS will permit to estimate this behavior and to decide if a thermal regulation would be required or not.

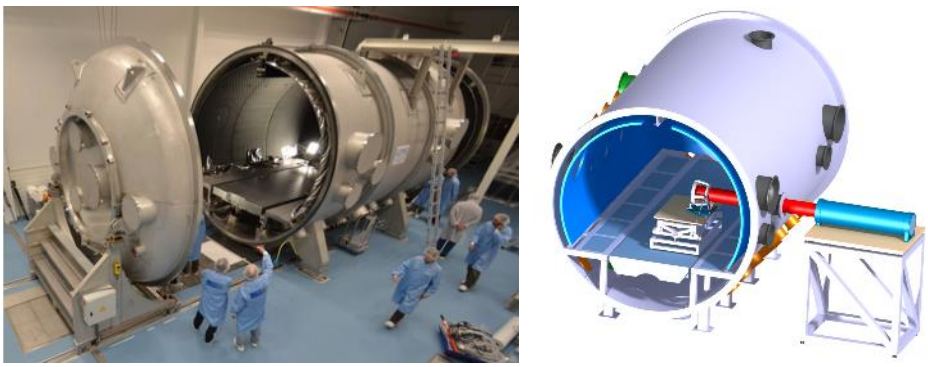

Figure 17. Left: ERIOS facility at LAM. Right: a preliminary concept of the thermal test bench

6.2 Optical test bench development

The strategy here is the use of an optical test bench located outside the ERIOS cryostat, in front of the window. The setup will include in particular an AIT slit to simulate the slit of the NIR-Spectrograph and an AIT spherical collimator mirror, both outside the cryostat. Figure 18 presents the optical layout including the camera inside the cryostat and the

pupil formed on the cryostat window.Indeed, the strategy here is to obtain the pupil on the window to facilitate the alignment of the prototype and the test phase with the bench; the distance between the camera prototype and the window will be determined consequently. This choice also contributes to reduce the manufacturing complexity, time and cost for the prototyping phase. The strategy for the NIR-Spectrograph science camera could differ by installing the NIR-Spectrograph slit and spherical collimator module inside ERIOS cryostat and to reproduce the same pupil size and distances than the nominal ones.

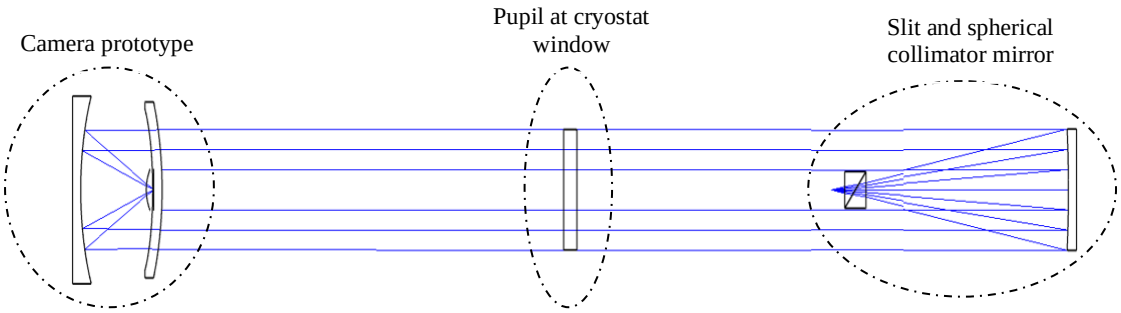

Figure 18. Layout of the optical test bench

The distance between the camera prototype and the pupil is approximately 1.5 m and driven by the available distance between the cryogenic bench and the cryostat window. With this configuration, the Field of View (FoV) is reduced by approximately factor 2 to be able to test the prototype without vignetting effect on the lens L1. This has no impact on the athermal behavior of the prototype and on the main objective of the tests but permits the use of a spherical collimator with a reduced diameter compared to the nominal one of the NIR-Spectrographs reaching double. The pupil positioned at the cryostat window allows minimizing the size of this window; the optical beam can also keep a fixed position on the window if the objected created by the slit moves angularly. The clear aperture of the window is approximately 260 mm.
The testing configuration is a double-path configuration using spherical reflectors in place of the detector. These reflectors will be glued on a dedicated dummy plate and positioned very precisely at the focal plane array (FPA) of the camera prototype. The optical beam is then reflected on these spheres towards the object plane, where a cube or a beamsplitter redirects the beam towards measurement tools. PSF measurement and wavefront sensing could be performed on-axis and in the field. The study and design of the detailed positioning way of the reflectors at FPA and of the global design of the dummy focal plane are in progress. The object will be created with a supercontinuum fibered source. Optical measurement will be performed using a CCD camera for PSF characterization (both in shape and in position) and wavefront measurement will be realized using a PHASICS sensor, located in a pupil plane and thanks to a second measurement arm. The preliminary layout is represented on Figure 19. After the first set of lenses, the CCD camera will be able to measure the focus behavior during the tests. The second set of lenses is ended by the wavefront sensor to measure the optical quality of the wavefront. Both measurements will be performed one after the other. The same test bench setup will be used to perform measurement before cooling (warm temperature) and after cooling. A monitoring during cool down and warm up sequences could also be considered. Alignment will be performed in Visible (633 nm) and in NIR-Infrared (1.2-1.3 µm) and optical measurement will be performed in NIR- Infrared.

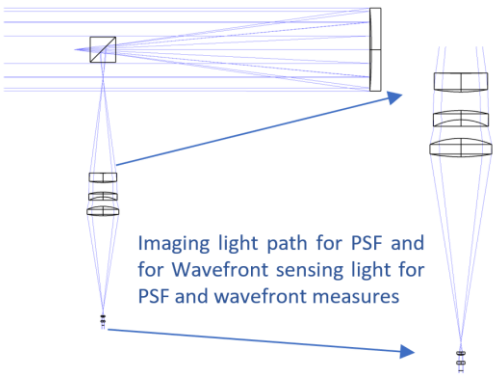

Figure 19. Optical arms located after the cube including PSF and wavefront measurement

7. CONCLUSION

The design of the camera prototype and of the optical test bench have evolved to be now compliant with a J-band working domain, according to the MOSAIC NIR-Channel evolution including now J-band and H-band observations. The prototype opto-mechanical design phase is close to the end. The optical design and the optical characteristics of the components also allow alignment and verification in the Visible to make easier this phase. From a thermo-mechanical point of view, design and calculations are very confident, based on strong expertise in cryogenic and space instruments. Results on the test campaign are also very confident regarding the selection of the gluing patterns and the dimensioning of the screwing, between each interface. Effort in progress is currently addressed to all the AIT tools and test benches dedicated to assemble and integrate the prototype and to perform optical and thermal tests. Final design on some of the assembly and integration tools is in progress. The optical test bench is well progressing and more efforts will be dedicated on the development of the thermal test bench in the next months. The manufacturing phase is expected to start at end 2024 for about one year duration and the prototype AIT is expected to start end-2025 at LAM. The AIT tools development is studied in a way to being able to be reused for the AIT steps of the final science cameras of the MOSAIC NIR spectrograph, identically or requiring little modifications and/or optimizations. This aspect is also in line with the efforts of the MOSAIC instrument team in the important topic of the reduction of the environmental impact in this kind of development ([7]). More generally, this athermal camera concept can also work over a very wide temperature range and can be suited for a large number of applications.

ACKNOWLEDGEMENTS

This work has received a funding support from the French "ANR-Programme d'Investissements d'Avenir", referenced as ANR-21-ESRE-0008 and from the French CSAA Program.
Part of this work is also developed in collaboration with Bertin Winlight (Bertin Technologies group, France).

REFERENCES

[1] Pello R., et al., "MOSAIC at the ELT: a unique instrument for the largest ground-based telescope", Proceedings of the SPIE, 13096-41 (2024, in preparation)
[2] Bharmal N., et al., "MOSAIC GLAO performance and system architecture: AO for the entire ELT focal plane", Proceedings of the SPIE, 13097-132 (2024, in preparation)
[3] Thurneysen M., et al., "Positioner using optical relay for the MOSAIC Instrument", Proceedings of the SPIE, 13096-214 (2024, in preparation)
[4] Floriot J., et al., "MOSAIC at ELT: the optical design of the NIR spectrograph", Proceedings of the SPIE, 13096-215 (2024, in preparation)
[5] El Hadi K., et al., "MOSAIC at the ELT front-end and instrument AITV planification", Proceedings of the SPIE, 13096-218 (2024, in preparation)
[6] Oliva E., et al., "Toward the final optical design MOONS, the Multi-Object Optical and Near infrared Spectrometer for the VLT", Proceedings of the SPIE, Volume 9908, id. 99087R 9 pp. (2016)
[7] Janssen A., et al., "Estimated environment impact of the ELT instrument MOSAIC", Proceedings of the SPIE, 13099-26 (2024, in preparation)
[8] Martin L., et al., "MOSAIC on the ELT: development of a camera prototype for the near-infrared spectrograph unit", Proceedings of the SPIE, Volume 12184, Ground-based and Airborne Instrumentation for Astronomy IX; 121848C (2022)